

Lab on a Chip

Accepted Manuscript



This is an *Accepted Manuscript*, which has been through the Royal Society of Chemistry peer review process and has been accepted for publication.

Accepted Manuscripts are published online shortly after acceptance, before technical editing, formatting and proof reading. Using this free service, authors can make their results available to the community, in citable form, before we publish the edited article. We will replace this *Accepted Manuscript* with the edited and formatted *Advance Article* as soon as it is available.

You can find more information about *Accepted Manuscripts* in the [Information for Authors](#).

Please note that technical editing may introduce minor changes to the text and/or graphics, which may alter content. The journal's standard [Terms & Conditions](#) and the [Ethical guidelines](#) still apply. In no event shall the Royal Society of Chemistry be held responsible for any errors or omissions in this *Accepted Manuscript* or any consequences arising from the use of any information it contains.



Journal Name

ARTICLE

A smart device for label-free and real-time detection of gene point mutations based on the high dark phase contrast of vapor condensation

Received 00th January 20xx,
Accepted 00th January 20xx

DOI: 10.1039/x0xx00000x

www.rsc.org/

Junqi Zhang,^{a†} Rongxin Fu,^{a†} Liping Xie,^{b†} Qi Li,^a Wenhan Zhou,^a Ruliang Wang,^a Jiancheng Ye,^a Dong Wang,^a Ning Xue,^a Xue Lin,^a Ying Lu,^a and Guoliang Huang^{*ac}

A smart device for label-free and real-time detection of gene point mutations related diseases was developed based on the high dark phase contrast of vapor condensation. The main components of the device included a Peltier cooler and a mini PC board for image processing. Heat from the hot side of the Peltier cooler causes the fluid in a copper chamber to evaporate, and the vapor condenses on the surface of a microarray chip placed on the cold side of the cooler. The high dark phase contrast of vapor condensation relative to the analytes on the microarray chip was explored. Combined with rolling circle amplification, the device visualizes less-to-more hydrophilic transitions caused by gene trapping and DNA amplification. Lung cancer gene point mutation was analysed, proving the high selectivity and multiplex analysis capability of this low-cost device.

Introduction

Gene mutations naturally occur in the human genome. In many cases, they can lead to highly fatal diseases, such as heart defects, metabolic disturbances, and cancer. Patients with such diseases are known to have a poor outcome. For example, nearly 75% of patients who suffer from cancer will die within 5 years¹. These diseases are difficult to diagnose at an early stage and thus usually do great harm to patients. Many types of cancer are closely related to gene point mutation. About 10% breast cancer cases in women are attributed to BRCA1 and BRCA2 mutations². Similarly, the tumorigenesis of lung epithelial cells is highly related to the abnormality of p53. Mutation of p53 tumor suppressor occurs in about 50% of non-small cell lung cancer (NSCLC)³. Most patients are not diagnosed before the cancer metastasis because its symptoms are hard to detect⁴. Therefore, it is important to detect gene mutations as early as possible.

Fortunately, great advances have been made in gene detection technology in recent years. Researchers have reported that for certain diseases resulting from genetic defects, the mutated gene can be detected via the blood, which provides many benefits for disease prevention and intervention⁵. Gene mutation examination is an important method for early

diagnosis and disease prevention, as well as a major medical service. Even if patients do not yet present any symptoms, the early diagnosis of cancer can greatly increase the chance for effective treatment and even a cure⁶.

Though gene mutation detection is useful for cancer diagnoses, detection devices are usually complicated and unaffordable for patients. Currently, many convenient and practical methods have been adopted to detect gene mutations, and yielded significant achievements⁷. Common detection methods include allele hybridization⁸, primer extension⁹, electrophoresis¹⁰, mass spectrometry¹¹, surface plasmon resonance¹², microfluidic chip¹³ and DNA sequencing¹⁴. However, one major obstacle is that these methods rely on fluorescence labelling and cannot work without expensive detection equipment. Progressive researches are also made in the recent years. Colorimetric DNA detection is well-developed but needs additional markers, such as modified gold nanoparticles¹⁵. Therefore, this method is not inherently a label-free process so that chemical transformation cannot be avoided fundamentally and superfluous detection steps are necessary. Other detection approaches are based on novel nanomaterial, such as carbon nanotube network¹⁶, silicon nanowires¹⁷, or nanochannel array¹⁸, but the preparation of nanomaterial needs professional skills so these methods are difficult to be widely applied. Optical reflection assay is also a commendable method, but gold-coated silicon AFM cantilevers is needed which is too expensive to be popularized¹⁹. Thus, in underdeveloped regions such as Asia, Africa and Latin America, such detection methods are not widely used due to their high cost. However, diseases linked to gene mutations are widespread in these regions. Therefore, developing a low-cost and easy-to-use device for early gene mutation analysis is of great value.

^a Department of Biomedical Engineering, Tsinghua University School of Medicine, Beijing 100084, China. E-mail: tshgl@tsinghua.edu.cn

^b College of Life and Health Science, Northeastern University, Shenyang 110004, China.

^c National Engineering Research Center for Beijing Biochip Technology, Beijing 102206, China.

[†] These authors contributed equally to this work.

[‡] Electronic supplementary information (ESI) available: For information on mill setup and alignment please see ESI. See DOI: 10.1039/xxxxxxxx

In this paper, we propose a portable smart device to realize early gene mutation detection, which combines the highly dark phase contrast of vapor condensation with rolling circle amplification (RCA). Formed by the accumulation of the condensation in natural air, small water droplets will scatter incident light. However, if the small droplets merge into a larger one, a water film will form and reflect light like a smooth surface²⁰. When observed against catoptric light, the spot where water film forms is more dazzling compared to surrounding areas due to the specular reflection. From a certain perspective, the high dark phase contrast of vapor condensation is formed because of different degrees of affinity to the condensed water, therefore, the image can be viewed at different brightness levels²¹. The DNA will collapse into a sphere and form hydrophilic DNA clusters through RCA. After exposed in airflow with certain humidity for a period of time, water film will form on the cold chip surface due to the RCA products and then brings about a high dark phase contrast. The proposed device takes full advantages of the hydrophilic RCA products and computer image processing technology to analyse the detection results²². The device is inexpensive, convenient, and highly sensitive, providing a new approach to detect gene point mutations.

Materials and methods

Detection principle

DNA molecules are hydrophilic, but the surface of the microarray chip is amino-modified silica²³, which has a lower affinity for water²⁴. A more hydrophilic surface shows stronger affinity toward water. As shown in (Fig. 1a-b), the chip after RCA have a higher wettability than the amino-modified silica, leading to a smaller water contact angle β (33.1°) than that α (49.5°) of the surface after probe immobilization. The RCA process produces more DNA, which improves the degree of wettability and enlarges the hydrophilic region. In a certain region where the RCA products exist, the hydrophilic clusters of RCA products will reflect light in a different way during vapour condensation, causing the high dark phase contrast of vapor condensation for visualization.

As shown in (Fig. 1c), the microarray chip consists of a Si basement and SiO₂ layer. When light illuminates the chip in a particular direction, more hydrophilic regions on the microarray chip reflect the light at a certain angle according to the law of reflection, but less hydrophilic regions scatter the light. When water vapor condensation occurs, the high dark phase contrast of vapor condensation can be visualised. If an image is taken from the direction of the reflection, the more hydrophilic regions will look brighter than the less hydrophilic regions. Referring to the microarray on the chip and the RCA process, if the capture DNA on the chip ligates the reporter DNA, the corresponding position will present a different brightness from the chip substrate²⁵. In this way, vapor condensation can be used to characterize the change on the surface, which is helpful to determine if a complementary base-pairing reaction has occurred.

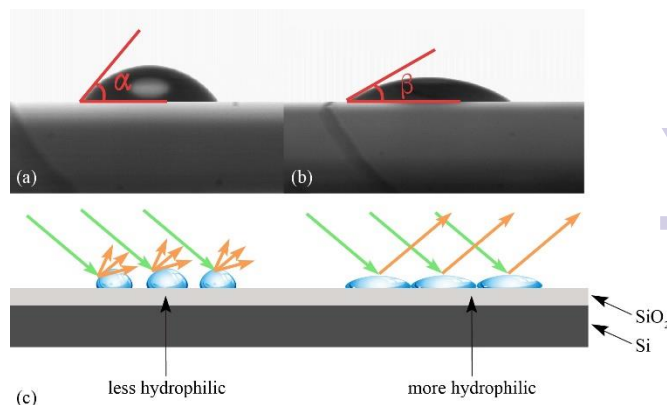


Fig. 1 (a) Water contact angle before RCA process. (b) Water contact angle after RCA process. (c) Different optical pathways when light illuminates less hydrophilic regions and more hydrophilic regions on the microarray chip.

With a macro lens to record video of the condensation process, a colour difference will be created due to the different affinities for water. A microprocessor can enhance the colour contrast and respond if a DNA cluster forms on the probe array. Then, the device will show if the gene mutation has occurred.

Water evaporation and vapor condensation

Vapor condensation and homogeneous nucleation are usually influenced by many factors, such as attributes of the substrate surface, the temperature on the substrate surface, and ambient humidity. To make the vapor condense quickly, the device uses a Peltier cooler to increase the air humidity and cool the microarray chip²⁶. The microarray chip is placed on the cold side of the cooler, and the Peltier cooler is placed in a copper sink (Fig. 2b). The device makes full use of the small component to form a heat and vapor cycle such that the hot side can increase the humidity, and the cool side can contribute to condensation. When a positive DC current is applied, electrons pass from the p-type semiconductor to the n-type semiconductor, and the temperature of the cold side decreases as the heat is absorbed²⁷. This heat is transferred to the hot side of the cooler (Fig. 2a), which is dissipated into the copper sink. The copper sink contains many cooling fins which are used to transfer heat away from the heat source to the liquid water faster and more efficiently. The liquid water changes to vapor when heated. Because it contacts the other side of the Peltier cooler, the microarray chip will quickly cool. Thus, water vapor will

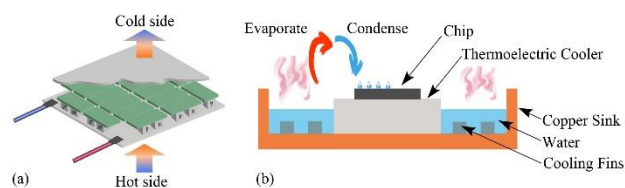


Fig. 2 Schematic illustration of the heat and vapor cycle. (a) Thermoelectric cooler. (b) Diagram of the heat and vapor transfer in the device.

condense into droplets on the surface of the microarray chip.

The overall structure

This device uses a pcDuino mini PC circuit as the core controller for the Peltier cooler, to collect videos, and to analyse images (Fig. 3a). The pcDuino controls the cooler by Pulse-Width Modulation (PWM), and a Metal-Oxide-Semiconductor Field-Effect Transistor (MOSFET). AO3416 is used to drive the high power Peltier cooler. With this method, the circuit system is small enough to be integrated, and the cooler can be smoothly operated. As the above-mentioned, the Peltier cooler is placed between the microarray chip and the copper sink. The device can transfer heat efficiently so that the microarray chip quickly cools when the cooler begins to work. The copper sink collects the heat from the hot side and transmits the heat to the water. Water evaporates when heated by the copper sink, and then vapor condenses at the surface of the microarray chip. The microarray chip is illuminated by a blue LED from the side face so that only scattered light from the chip can be collected by the

macro lens. The image of the microarray chip is gathered through the macro lens (Fig. 3b), and the results are outputted through a process of colour contrast enhancement by the core controller (Fig. 3c). We can easily detect the high dark phase contrast of vapor condensation if RCA products have been generated on the microarray chip.

Microarray chip, DNA ligation, and RCA process

The microarray chip is based on a silicon substrate with a 680-nm-thin SiO₂ film on its surface. The film was synthesized on the silicon substrate by thermal oxidation²⁸. The chip was first cleaned by oxygen plasma. Then, the chip is cut into the designed size and placed in 6% 3-Aminopropyltrithoxysilane (APTES) ethanol solution for 1 h. After washed with deionized water and dried under nitrogen, the chip was amino-modified to provide extra affinity between the SiO₂ film and DNA molecules²⁹. DNA primers were spotted on the surface of chip using a SmartArray48 microarray spotter (CapitalBio, China) depending on the needs of the experiment. The concentration of all primers was 5 μmol/L³⁰.

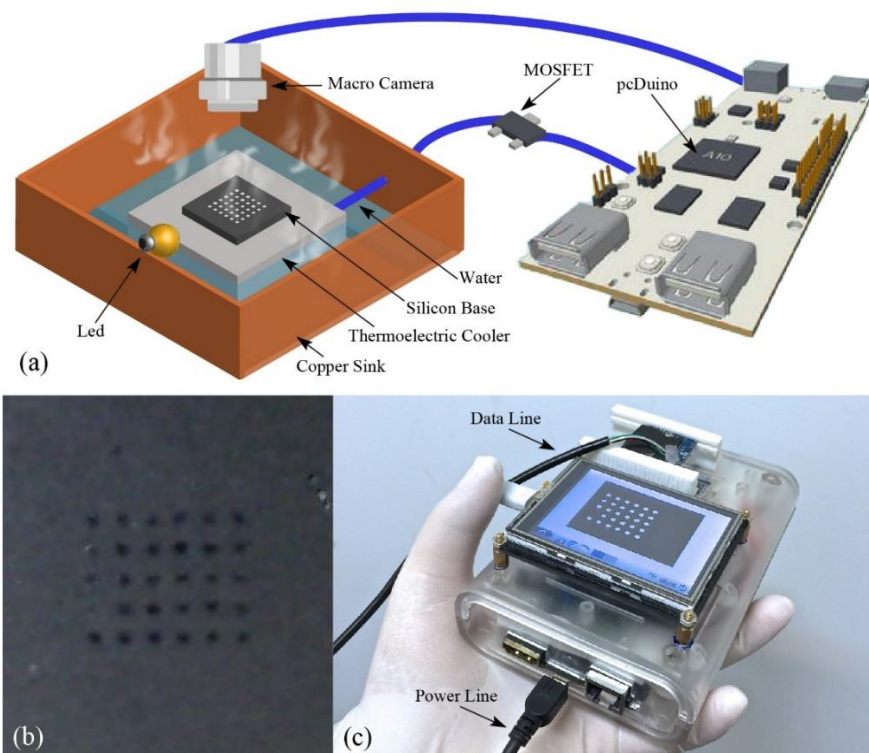


Fig. 3 Setup of the device to detect gene point mutations based on vapor condensation. (a) Structural schematic of the device. (b) Image of high dark phase contrast. (c) Actual picture of the whole device.



Journal Name

ARTICLE

To discriminate a short DNA sequence with a single-base mismatch, we integrated target induced DNA ligation. The chip was washed with 10% PBST solution and deionized water twice after the capture DNA was spotted on the chip by the spotter (Fig. 4a). To specifically detect the point mutation, the biochemical activity of the *Taq* DNA ligase enzyme was exploited. Bridged by target DNA, reporter probe will be ligated to the capture probe in the presence of *Taq* DNA ligase, if and only if the capture probe accurately matches the target DNA around the mutation site, to form a long ssDNA, which was designed to be the primer for RCA (Fig. 4b).

As the concentration of the lengthened single-stranded DNA is usually very low, an amplification step is needed to enlarge the hydrophilic region to permit visualization. RCA is a simple, highly sensitive, and specific process in which a short DNA primer can be amplified using a circular DNA template and special DNA polymerases. The product of RCA is a concatemer containing 10s to 100s of tandem repeats, making them easier to detect. Moreover, RCA process can be carried out easily at room temperature, which makes complex temperature control system unnecessary³¹.

A 30-min incubation at 60°C and another 30 min at 25°C are needed to bind the reporter DNA and the pre-loop template DNA. Then, 5 μL 4.5 μM pre-loop template DNA, 8 U/μL T4 DNA ligase, and buffer mixture were added to each microarray. After incubation at room temperature for 4 h, the two ends of the pre-loop templates will connect, forming loop template for the following RCA (Fig. 4d). The RCA reaction buffer includes 40 mM Tris-HCL (pH=7.5), 50 mM KCl, 10 mM MgCl₂, 5 mM (NH₄)₂SO₄,

4 mM DDT, 5 U/μL Phi29 DNA ligase, and 880 μM dNTPs. RCA reaction buffer (5 μL) was added to the surface, and the chip was incubated at 30°C for 4 h. At that point, the DNA clusters will have formed (Fig. 4e). In the electronic supplementary information, we have showed the whole workflow (Fig. S2). The portable device shown in (Fig. S3) is used to control the temperature and detect the mutation signals. All the process illustrated in Fig. 4 can be carried out in the device.

Results

To test and verify the feasibility of this device, DNA was amplified on the surface of the microarray chip by RCA, and then the microarray chip was observed and analysed with the proposed device. As shown in Fig. 5a, the sequence of the primer in the first six columns was ssDNA1, and the sequence of the primers in the other three columns was ssDNA2. The template that matches the sequence of primer in the first six columns can form a circular oligonucleotide in the presence of resulted in a bright signal, so we concluded that the RCA products can be detected with this device. Specific ssDNA can be identified clearly after RCA and image processing (Fig. 5d). The results of the SYBR fluorescent staining on the chip are consistent with our expectations (Fig. 5e). In electronic supplementary information, a hyperspectral interference imaging is also showed as comparative results (Fig. S1b). The interference microscope is proposed in reference 23.

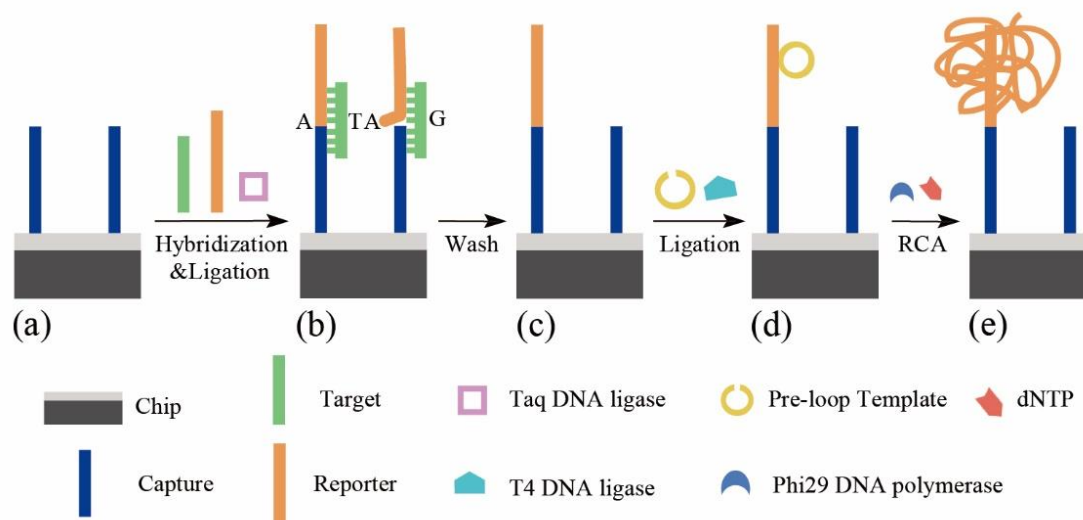


Fig. 4 Reaction scheme of the DNA ligation and RCA. (a) Microarray chip, (b) specific hybridization, (c) ligation after washing, (d) RCA, and (e) DNA clusters after RCA.

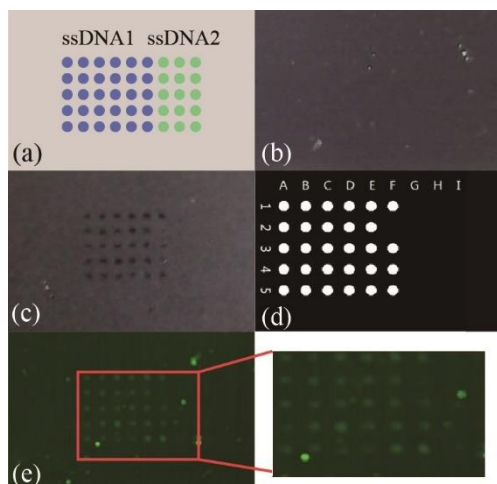


Fig. 5 DNA network amplified by RCA resulting in a less-to-more hydrophilic transition. (a) A 5×9 microarray containing two types of ssDNA. (b) Chip before vapor condensation. (c) Chip after vapor condensation. (d) Image after processing and distinguishing. (e) Comparative results of fluorescence microscopy.

In this experiment, the size of the chip was 3 mm×5 mm, and the DNA primer array was of the 5×9 type. With a diameter of only 50 μm, every primer spot is 200 μm away from the other spots.

To determine how long it takes to adequately enhance the contrast between less hydrophilic regions and more hydrophilic regions, we performed a series of experiments. By comparing the image at different times, we found that the best condensation effect was achieved at approximately the 10th second. The 10 seconds include the time duration after the LED turning on, the exposure time of camera, work time of the peltier, and the time to generate vapour. We thus chose the image at 10 s for subsequent processing (Fig. 6).

The ability to discriminate between a fully complementary target and a sequence with a single-base mismatch is important for many biomedical applications like screening for genetic diseases. To test and verify the high sensitivity, specificity, and multiplex ability of the detection system, we chose synthesized



Fig. 6 Condensation at different times. (a) Image at 3 s, (b) 6 s, and (c) 10 s.

target DNA sequences, which were designed according to the three types of predominant mutations (CGT→CAT, CGT→CTT, and CGT→CCT) at codon 273 of p53 in lung cancer patients. Detailed DNA sequence information is shown in the electronic supplementary information.

First, four types of capture probes were spotted onto the microarray chip using the spotter (Fig. 7a). For each chip, only one type of target mutation sequence was added. During the detection process, the hydrophilic characteristics of the DNA change the hygroscopic characteristics of the microarray surface, so we can easily observe dynamic changes of the microarray using the device proposed in this paper. The results are shown in (Fig. 7b-e). Proof-of-concept detection of synthesized 27-mer ssDNA target (a single-base mismatch at codon 273 of p53, CGT→CAT, CGT→CTT, and CGT→CCT) was accomplished which validated the usefulness of this platform. The concentration of point mutation sequence is 1 μM (Sangon Biotech, China), which can be easily extracted from the blood sample using commercial kit (CapitalBio, China).

Conclusion and discussion

In this paper, a label-free, water-enabled, on-chip DNA assay device was proposed that can be used to detect gene point mutations. Indeed, we built an inexpensive, portable device to detect gene point mutations based on this strategy. Unlike existing commercial instruments, this device is only qualitative, but it does not rely on expensive equipment, enabling people in underdeveloped regions to diagnose genetic diseases. According to the above experiments, the device can detect gene point mutations rapidly, specifically, and with high sensitivity. Our results also prove that this low-cost device can be used to detect genetic diseases even when only one point mutation has occurred. Combined with the advantages of microarray chips, a high-throughput, parallel melting, and rapid method can be achieved.

This device makes full use of the electric-thermal characteristics of Peltier cooling to form a thermal cycle. Additionally, with the image processing ability of the mini-PC circuit, it can automatically judge and visualize diagnosis results. The whole device is as small as a common mobile phone, making it portable and convenient, which is beneficial for commercial promotion. The device can be used as a preliminary qualitative detection tool in medical examinations or clinically.

Acknowledgments

This work was supported by the National Natural Science Foundation of China (81327005, 61361160418), the National

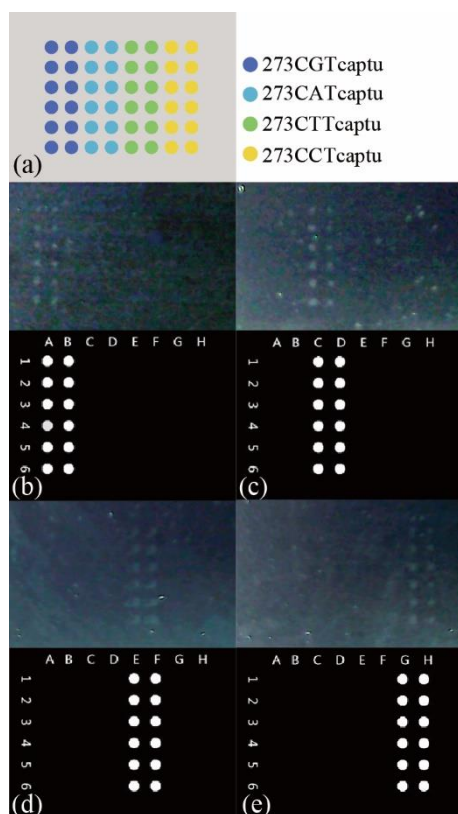


Fig. 7 Multiplex gene point mutation detection. (a) Array of the capture probe. (b)-(e) Images of detection of wild type sequence (CGT) and mutations (CGT→CAT, CGT→CTT, and CGT→CCT) on the chip after DNA ligation, RCA, and vapor condensation.

Foundation of High Technology of China (2012AA020102, 2013AA041201), the Projects 973 of China (2011CB707701), the National Key Foundation for Exploring Scientific Instruments (2013YQ190467), the Beijing Municipal Natural Science Foundation (4142025), the Beijing Lab Foundation, the Tsinghua Autonomous Research Foundation (2014Z01001), and the Tsinghua Lab Innovate Foundation (110020003).

References

- 1 T. Kosaka, Y. Yatabe, H. Endoh, H. Kuwano, T. Takahashi and T. Mitsudomi, *Cancer Research*, 2004, **64**, 8919.
- 2 A. C. Antoniou, P. D. P. Pharoah, G. McMullan, N. E. Day M. R. Stratton, J. Peto, B. J. Ponder and D. F. Easton, *Brit. J. Cancer*, 2002, **86**, 76.
- 3 S. P. Hussain, P. Amstad, K. Raja, S. Ambs, M. Nagashima, W. P. Bennett, P. G. Shields, A. Ham, J. A. Swenberg, A. J. Marrogi and C. C. Harris, *Cancer Research*, 2000, **60**, 3333.
- 4 T. Soussi, and C. Bérout, *Nat. Rev. Cancer*, 2001, **1**, 233.
- 5 L. Z. Rassenti, L. Huyuh, T. L. Toy, L. Chen, M. J. Keating, J. G. Gribben, D. S. Neuberg, I. W. Flinn, K. R. Rain, J. C. Byrd, N. E. Kay, A. Greaves, A. Weiss and T. J. Kipps, *New Engl. J. Med.*, 2004, **351**, 893.
- 6 R. A. Smith, A. C. von Eschenbach, R. Wender, B. Levin, T. Byers, D. Rothenberger, D. Brooks, W. Creasman, C. Cohen, C. Runowicz, D. Saslow, V. Cokkinides and H. Eyre, *CA-Cancer J. Clin.*, 2001, **51**, 38.
- 7 R. K. Thomas, A. C. Baker, R. M. DeBiasi, W. Winckler, T. LaFramboise, W.M. Lin, M. Wang, W. Feng, T. Zander, L. E.

- MacConaill, J. C. Lee, R. Nicoletti, C. Hatton, M. Goyette, L. Girard, K. Majmudar, L. Ziaugra, K. Wong, S. Gabriel, R. Beroukhir, M. Peyton, J. Barretina, A. Dutt, C. Emery, H. Greulich, K. Shah, H. Sasaki, A. Gazdar, J. Minna, S. A. Armstrong, I. K. Mellinghoff, F. S. Hodi, G. Dranoff, P. S. Mischel, T. F. Cloughesy, S. F. Nelson, L. M. Liao, K. Mertz, M. A. Rubin, H. Moch, M. Loda, W. Catalona, J. Fletcher, S. Signoretti, F. Kaye, K. C. Anderson, G. D. Demetri, R. Dummer, S. Wagner, M. Herlyn, W. R. Sellers, M. Meyerson and L. A. Garraway, *Nature Genetics*, 2007, **39**, 347.
- 8 R. H. Hruban, A. D. van Mansfeld, G. J. Offerhaus, D. H. van Weering, D. C. Allison, S. N. Goodman, T. W. Kensler, K. K. Bose, J. L. Cameron, and J. L. Bos, *Am. J. Pathol.*, 1993, **143**, 545.
- 9 J. M. Schumaker, A. Metspalu and C. T. Caskey, *Human Mutation*, 1996, **7**, 346.
- 10 R. Fodde and M. Losekoot, *Human Mutation*, 1994, **3**, 83.
- 11 A. Braun, D. P. Little and H. Köster, *Clin. Chem.*, 1997, **43**, 1151.
- 12 S. Chen, T. Deng, T. Wang, J. Wang, X. Lin and G. Huang, *J. Biomed. Opt.*, 2012, **17**, 0150051.
- 13 G. Huang, C. Wang, L. Ma, X. Yang, X. Yang and G. Wang, *Anal. Chim. Acta.*, 2011, **685**, 1.
- 14 R. A. Gibbs, P. N. Nguyen, L. J. McBride, S. M. Koepf, and C. T. Caskey, *PNAS*, 1989, **86**, 1919.
- 15 W. Xu, X. Xie, D. Li, Z. Yang, T. Li and X. Liu, *Small*, 2012, **8**, 1846.
- 16 A. Star, E. Tu, J. Niemann, G. P. Gabriel, C. S. Joiner and C. Valcke, *PNAS*, 2006, **103**, 921.
- 17 Z. Li, Y. Chen, X. Li, T. I. Kamins, K. Nauka and R. S. Williams, *Nano Lett.*, 2004, **4**, 245.
- 18 S. Li, J. Li, K. Wang, C. Wang, J. Xu, H. Chen, X. Xia and Q. Huo, *ACS Nano*, 2010, **4**, 6417.
- 19 K. Hansen, H. Ji, G. Wu, R. Datar, R. Cote, A. Majumdar, T. Thundat, *Anal. Chem.*, 2001, **73**, 1567.
- 20 M. He, A. S. Blum, D. E. Aston, C. Buenviaje, R. M. Overney and R. Luginbühl, *J. Chem. Phys.*, 2001, **114**, 1355.
- 21 N. Martel, S. A. Gomes, I. Chemin, C. Trépo and A. Kay, *J. Virol Methods*, 2013, **193**, 653.
- 22 Q. Huang, S. Han, Y. Zhang, X. Qu, J. Fu, Z. Z. L. Ding, Y. Qian, X. Zhao and G. Huang, *J. Comput. Theor. Nanos*, 2015, **12**, 1-6.
- 23 T. Wang, Q. Li, S. Zhao, Y. Lu and G. Huang, *Opt. Lett.*, 2013, **38**, 1524-1526.
- 24 Y. Bai, M. Song, Y. Cui, C. Shi, D. Wang, G. C. Paoli and X. Shi, *Anal. Chim. Acta.*, 2013, **787**, 93-101.
- 25 B. Wang, C. He, C. Tang and C. Yin, *Biomaterials*, 2011, **32**, 4630-4638.
- 26 A. R. McLanahan, C. D. Richards, and R. F. Richards, *J. Micromech. Microeng.*, 2011, **21**, 104009-104020.
- 27 N. Mukhitov, L. Yi, A. M. Schrell and M. G. Roper, *J. Chromatogr. A*, 2014, **1367**, 154-160.
- 28 D. A. Markov, K. Swinney and D. J. Bornhop, *JACS*, 2004, **126**, 16659-16664.
- 29 Q. Li, K. Zhang, T. Wang, X. Zhou, J. Wang, C. Wang, H. Lin, X. Li, Y. Lu and G. Huang, *Analyst*, 2012, **137**, 3760-3766.
- 30 T. Wang, L. Xie, H. Huang, X. Li, R. Wang, G. Yang, Y. Du and G. Huang, *Chinese Opt. Lett.*, 2013, **11**, 111102.
- 31 G. Huang, Q. Huang, L. Ma, X. Luo, B. Pang, Z. Zhang, R. Wang, J. Zhang, Q. Li, R. Fu and J. Ye, *Scientific Reports*, 2014, **4**, 7344.